Journal of Solid State Electrochemistry (2025) 29:1449–1458
https://doi.org/10.1007/s10008-024-06114-y

ORIGINAL PAPER

Tuning the geometry of porous alumina layers via anodization in mixtures of different acids

Aleksandra Świerkula[1,2] · **Leszek Zaraska**[1]

Received: 31 July 2024 / Revised: 26 September 2024 / Accepted: 14 October 2024 / Published online: 22 October 2024

Abstract

Porous anodic aluminum oxide (AAO) layers have been obtained by two-step anodization of high-purity Al in two types of acid mixtures, i.e., in $H_2C_2O_4$–H_3PO_4 and, for the first time, in H_2SO_4–H_3PO_4 systems. The kinetics of oxide formation was examined by monitoring the current vs. time curves while the morphology of the resulting layers was carefully verified by scanning electron microscopy (SEM). A special emphasis was put on establishing correlations between electrolyte composition, the kinetics and effectiveness of oxide growth, and the morphological features of AAO layers (pore and cell diameter, porosity), as well as pore arrangement. It was confirmed that the addition of H_3PO_4 to both $H_2C_2O_4$ and H_2SO_4 electrolytes results in a significant decrease in oxide growth rate, and worsening of pore arrangement, while the values of pore diameter and interpore distance are much less affected. Moreover, the presence of a small amount of phosphoric acid in the reaction mixture allowed for a noticeable increase in pore ordering if anodization was carried out beyond the self-ordering regime, or performing controlled anodization even at voltages at which the burning phenomenon is typically observed. It is strongly believed that manipulating the electrolyte composition by adding another acid may provide another degree of freedom to control the morphology of the resulting nanostructured alumina layers.

Keywords Anodic alumina · Anodization · Acidic electrolytes · Acid mixtures

Introduction

Porous anodic aluminum oxide (AAO) has been considered for several decades as a very promising and versatile material for many important applications including template-assisted fabrication of various types of nanostructures [1, 2], decorative coatings [3], filtration systems [4], sensing devices [5], chromatography [6], biomedical applications [7], and many others [8].

Among many advantages of AAO, the possibility to control its morphology (including pore diameter and shape, pore-to-pore spacing, pore density, porosity, the overall oxide layer thickness, etc.) by simple adjusting conditions applied during the electrosynthesis process, seems to be especially important. Moreover, under appropriately selected anodization conditions, it is possible to obtain well-defined porous oxide films with hexagonally ordered channels [9, 10].

Hundreds of papers describing the correlations between anodizing conditions and morphological parameters of AAO films have been already published [8–10]. It is well known that the most important factors affecting the morphology of nanostructured Al_2O_3 layers are the type of electrolyte used and the voltage applied during electrolysis [9, 11]. In addition, the type of electrolyte also determines the voltage range, in which the best hexagonal pore order can be achieved. These ranges are called self-ordering regimes and are specified for the particular electrolytes, e.g., 19–25 V for sulfuric acid, 35–45 V for oxalic acid, and 165–195 V for phosphoric acid to mention only those most commonly used [9–11]. However, when the voltage beyond the self-ordering regime is applied during the anodization, a less ordered porous structure is formed [12]. Moreover, when the process is carried out at too high voltage, electrochemical dissolution of the metallic Al is observed instead of controlled growth of oxide film on its surface. One of the strategies to extend

✉ Leszek Zaraska
leszek.zaraska@uj.edu.pl; zaraska@chemia.uj.edu.pl

[1] Faculty of Chemistry, Department of Physical Chemistry and Electrochemistry, Jagiellonian University, Gronostajowa 2, Krakow 30-387, Poland

[2] Doctoral School of Exact and Nature Science, Jagiellonian University, Prof. S. Łojasiewicza 11, Kraków 30-348, Poland

the voltage range at which porous AAO can be formed in particular acid is the addition of a nonaqueous solvent to the electrolyte to decrease the conductivity of the solution [10, 13].

In the vast majority of cases, the Al anodizing is carried out in the electrolytes containing one type of acid [10]. However, several attempts to use mixtures of different acids as electrolytes for anodization have been also made to verify whether and how the combination of two different acids affects the morphology and kinetics of growth of the AAO layer. The application of such electrolytes might make it possible to obtain layers showing self-ordering at voltages beyond the optimal ranges for pure acids, as well as to change the morphological features of the resulting oxide films. So far, among others, mixtures of malonic and sulfuric acid [14, 15], oxalic and phosphoric acid [16–23], or citric and phosphoric acid [24–26] have been proposed as electrolytes for Al anodization. Moreover, much attention has been also paid to a mixture of oxalic and sulfuric acid [27–34]. Nevertheless, systematic studies on the effect of the composition of the acid mixture on the morphological features and, especially, the kinetics of the entire oxide layer growth and degree of pore order have not been performed so far. Finally, Yanagishita et al. [35] reported that the addition of a small amount of H_3PO_4 to the electrolyte results in better uniformity of the thickness of AAO films obtained in extremely dilute H_2SO_4. However, surprisingly, no other research has systematically investigated the use of a mixture of sulfuric and phosphoric acid as an electrolyte for Al anodization.

Therefore, herein we tried to fill the aforementioned gaps by performing a series of anodizations of high-purity Al substrate in two types of acid mixtures: (i) $H_2C_2O_4$ – H_3PO_4 (series A) and (ii) H_2SO_4 – H_3PO_4 (series B). Special attention was focused on the effect of electrolyte composition (the ratio of the concentrations of individual acids) on the kinetics and effectiveness of the oxide growth, morphological parameters of the resulting layers, and pore arrangement. It has been proven that manipulating the electrolyte composition by adding another acid may provide another degree of freedom to control the morphology of the resulting nanostructured alumina layers.

Experimental

Samples pre-treatment

High-purity aluminum foil (purity: 99.999%, Goodfellow, thickness: 0.5 mm) was used as a starting material. First, the Al foil was cut into specimens with a size of 1×3 cm which were cleaned with ethanol and air-dried. In the next step, the samples were electrochemically polished in a mixture of perchloric acid (60%) and ethanol (1:4 vol.) at the constant voltage of 20 V for 30 s at a temperature of 0 °C. The platinum mesh was used as a cathode. After polishing, the plates were rinsed in distilled water and ethanol and air-dried. Finally, the working surface of the electrode (approx. 1 cm^2) was defined by an acid-resistant paint.

Two-step anodization

Al samples were subjected to two-step anodization. The process was carried out in a double-walled electrochemical cell placed on a magnetic stirrer and connected to a thermostat (Thermo Haake, DC10-K14). A lead plate with a working surface area of 6 cm^2 was used as the cathode. The distance between the electrodes was approximately 2 cm. The process was carried out in 0.3 M $H_2C_2O_4$, 0.3 M H_2SO_4, 0.3 M H_3PO_4, and mixtures of these acids of various compositions. Different sets of anodizing conditions (temperature, voltage, and duration of the process) were applied depending on the electrolyte used. All anodizing conditions were collected in Tables S1 and S2 in the Supplementary Information. Details are also provided in the following sections. Oxide layers formed during the 1st step of anodization were removed in a mixture of 6 wt% phosphoric acid and 1.8 wt% of chromic acid at a temperature of 60 °C for 2 h. The current-time curves were recorded using an APPA207 multimeter.

Samples characterization

The morphology of the obtained layers was verified by a field-assisted scanning electron microscope (Hitachi S-4700). The morphological parameters of the oxide films were determined directly from the SEM images by using ImageJ v. 1.37 [36], WSxM v. 12.0 [37] software, and dedicated executable software according to the methodology developed in our group [12, 38, 39].

Results and discussion

Anodization of Al in $H_2C_2O_4$ – H_3PO_4 mixtures

In the first step of the research, various electrolytes with different contents of oxalic acid and phosphoric acid were used for Al anodizing. Current density vs. time curves recorded during anodizations at all studied conditions are collected in Fig. 1.

As can be seen, no matter which voltage was applied during the anodization, the same tendency is maintained. The more phosphoric acid in the mixture, the lower the current flowing through the sample and, in consequence, the lower charge passing through the system during the whole process (see Fig. S1 in the Supplementary Information). Moreover,

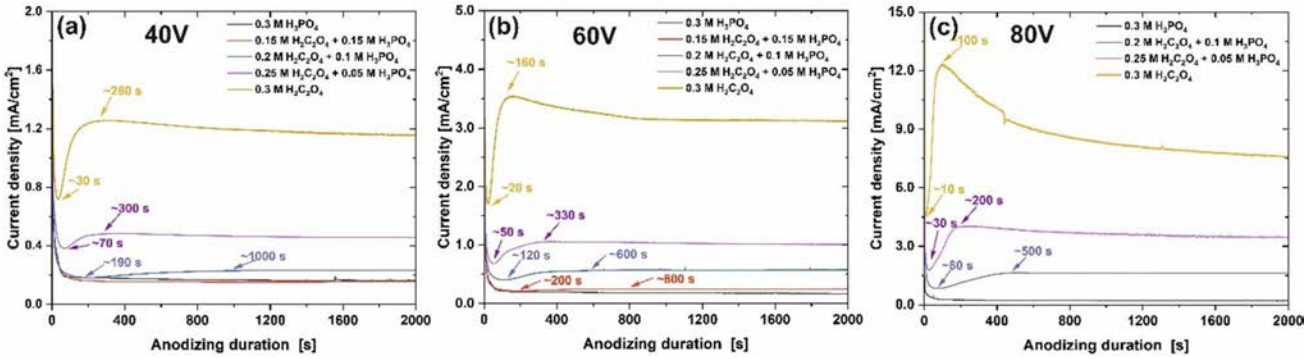

Fig. 1 Current density vs. time curves recorded during the first 2000 s of 2nd anodization steps carried out in electrolytes based on $H_2C_2O_4$ and H_3PO_4 of different compositions at the potential of 40 V (**a**), 60 V (**b**), and 80 V (**c**)

the shape of the curve changes drastically when the electrolyte composition is altered. It is generally accepted [8–10] that the initial rapid current drop during the first few seconds of the process is related to the formation and gradual thickening of the compact oxide layer on the metal surface. After some time, the local minimum of the current is achieved and a noticeable current increase is observed as evidence of the generation of pore embryos in the compact oxide film (possible mechanisms of pore formation have been already discussed by other authors [8–10]). Subsequently, the current reaches a stable value which indicates that the steady-state oxide growth was attained.

As can be seen, in the case of using pure phosphoric acid as an electrolyte, the shape of the curve rather resembles those observed for the formation of passive oxide layers. A small minimum of current density is indeed noticeable, but it is very wide and difficult to isolate as a separate point. It means that the process of pore formation is very slow, which is in line with expectations since the studied potentials are far away from the self-ordering regime for pure H_3PO_4. On the other hand, the addition of oxalic acid to the electrolyte causes a local minimum to gradually appear on the current curve. The more oxalic acid in the electrolyte and the higher the anodizing voltage, the earlier this minimum is achieved, indicating the faster formation of the pores (note that the steady-state oxide growth is also attained faster). What is interesting, the shape of the current vs. time curve as well as the values of currents observed for the electrolyte containing 0.15 M $H_2C_2O_4$ and 0.15 M H_3PO_4 and pure 0.3 M H_3PO_4 are almost the same, especially when the process is carried out at 40 V. It means that the excess of oxalic acid is required to significantly affect the anodic formation of AAO layers (see also below). Finally, when pure $H_2C_2O_4$ was used as an electrolyte, the local current maximum was also observed on the current vs. time curve. This phenomenon is commonly attributed to the reorganization of the pores, i.e., merging of the initially formed channels into larger ones that result in a gradual decrease of the current before the steady-stade growth is achieved [8–10]. The observed trends are strongly in line with the previous works [40] showing that changing any anodizing parameter (e.g., potential, temperature) that results in an increase of the current density (i.e., the reaction rates) leads to the faster formation of the nanochannels within the oxide layer.

Figure 2 shows SEM images of the surfaces and cross-sections of selected layers obtained in different electrolytes based on both acids. The differences between the layers obtained in different electrolytes are clearly visible. Firstly, the more phosphoric acid in the electrolyte, the thinner the layers formed, which of course correlates well with the lower values of the charge flowing through the system (Fig. S1 in the Supplementary Information). Importantly, even the presence of 0.05 M phosphoric acid in the mixture results in a decrease in the oxide growth rate by more than half compared to pure oxalic acid. Additionally, if the electrolyte contains an equimolar mixture of acids, the differences between the layers obtained in this electrolyte and those grown in pure phosphoric acid are very small (see Fig. 3a). The oxide growth ratio defined as the ratio of the layer thickness to the total charge density was also calculated for all studied samples. It was generally found that the higher the H_3PO_4 content in the electrolyte, the lower the oxide growth ratio (except for the sample for 60 V for an equimolar acid mixture) (Fig. 3a), but it must be remembered that this parameter is not identical with the growth efficiency, because it does not take into account the morphological differences between the layers, in particular the porosity of the films obtained under different conditions. It should be also noticed that the channels formed in pure $H_2C_2O_4$ are oriented perpendicularly to the Al surface, however, those generated in AAO layers formed in H_3PO_4 are slightly tilted as can be seen in Fig. 2f (see inset). Moreover, some small branches within the channels can be also recognized. The process of the formation of such kind of tilted and serrated channels in phosphoric acid electrolytes has been described in our previous work [41] as well by other authors [42, 43].

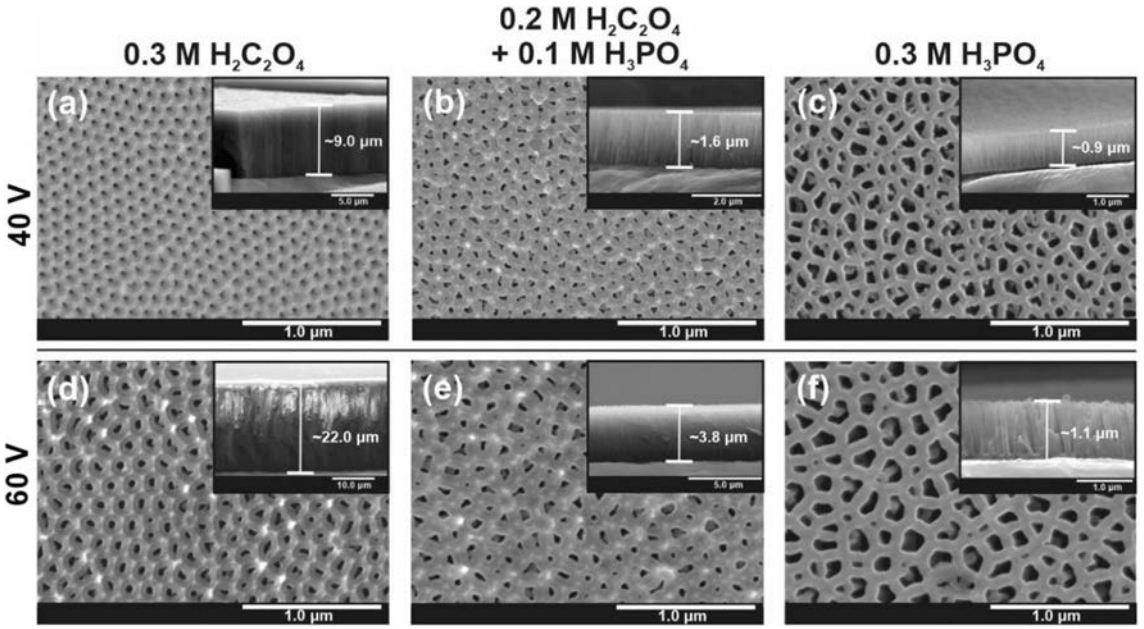

Fig. 2 FE-SEM images of AAO layers grown by two-step anodization in various electrolytes and different applied voltages (cross-sectional views shown as insets)

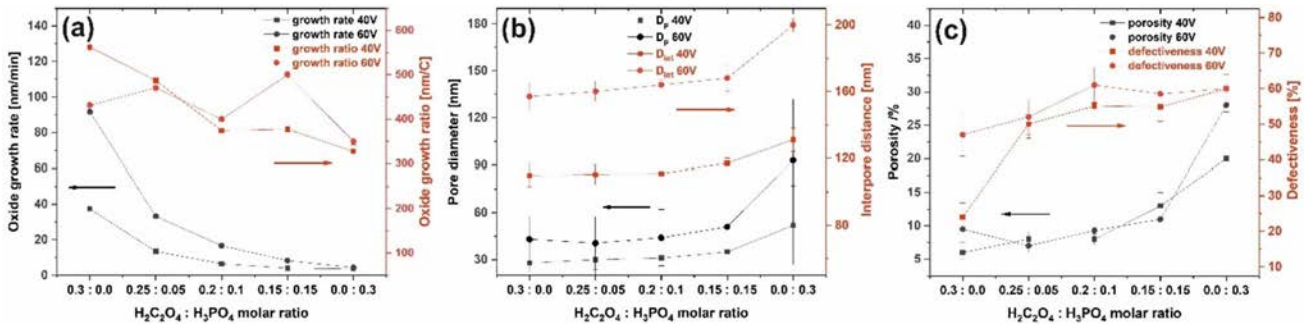

Fig. 3 The values of oxide growth rate and oxide growth ratio (**a**), average pore diameter and interpore distance (**b**), average porosity and percentage of defective pores (**c**) calculated for porous AAO layers grown in electrolytes of different content of $H_2C_2O_4$ and H_3PO_4 at 40 V and 60 V

A brief analysis of SEM images indicates that the higher the phosphoric acid content in the electrolyte, the larger and more inhomogeneous the pores within the anodic film, which is confirmed by the larger standard deviations (see Fig. 3b). Similarly, the more phosphoric acid, the slightly larger the distances between pores (cell sizes – D_c). While it is generally known that the main anodization parameter determining D_c is the voltage applied during the process, the increase in D_c with the change in the electrolyte composition can be explained by the lower degree of pore order (see below) and the decrease in pore distribution uniformity. However, it should be emphasized that while the rate of growth is significantly dependent on the phosphoric acid content, the D_p and D_c values determined for AAO films grown at 40 V and 60 V in all electrolytes containing $H_2C_2O_4$ are relatively similar (see Fig. 3b). The result of the trends described above (especially changes in the D_p value) is the observed increase in the porosity of the layers with the increase in the phosphoric acid content (see Fig. 3c).

The degree of hexagonal pore order was estimated by calculation of the percentage of defective pores, defined as a ratio between the number of non-six-fold coordinated pores to the total number of pores on the analyzed surface (details of the methodology were presented in our earlier works [12, 39, 44]). As expected, the best hexagonal pore arrangement was observed for the AAO layer obtained in pure $H_2C_2O_4$ at 40 V (self-ordering regime). With the addition of phosphoric acid to the electrolyte, a dramatic increase in the defectiveness was observed (see Fig. 3c), however, the differences were less pronounced for samples anodized at

60 V (i.e., beyond the self-ordering regime). The observed trend is consistent with the expectations (the self-ordering regime for phosphoric acid is about 195 V). The degree of pore order was also assessed on the basis of FFT transforms according to the methodology developed in our group [45, 46]. The obtained results (not shown here) confirmed the trend described above.

Since the potential of 40 V is the self-ordering regime for oxalic acid, and 60 V is quite close to the self-ordering regime [9], it was decided to carry out anodization at 80 V, i.e. at the potential when a noticeably worse degree of pore order is typically achieved in pure oxalic acid [12]. Figure 4 shows SEM images of the surfaces and cross-sections of films obtained at 80 V in electrolytes with different contents of both acids. It is clearly visible that the trends observed for voltages of 40 and 60 V are also preserved, i.e. the more phosphoric acid in the electrolyte, the slower the oxide growth, the lower the growth efficiency, and the larger the distances between pores as shown in Fig. 5 (note that the D_c values obtained for layers anodized in H_3PO_4 solution are strongly in line in the previous works [10]). However, neither the pore diameters nor the porosity changed significantly after the addition of 0.1 M phosphoric acid to the electrolyte. Moreover, the analysis of the degree of pore order allows us to state that slightly less defective (however within the uncertainty) channels were observed for the sample anodized in mixtures containing 0.05 M and even 0.1 M phosphoric acid compared to this formed in pure $H_2C_2O_4$

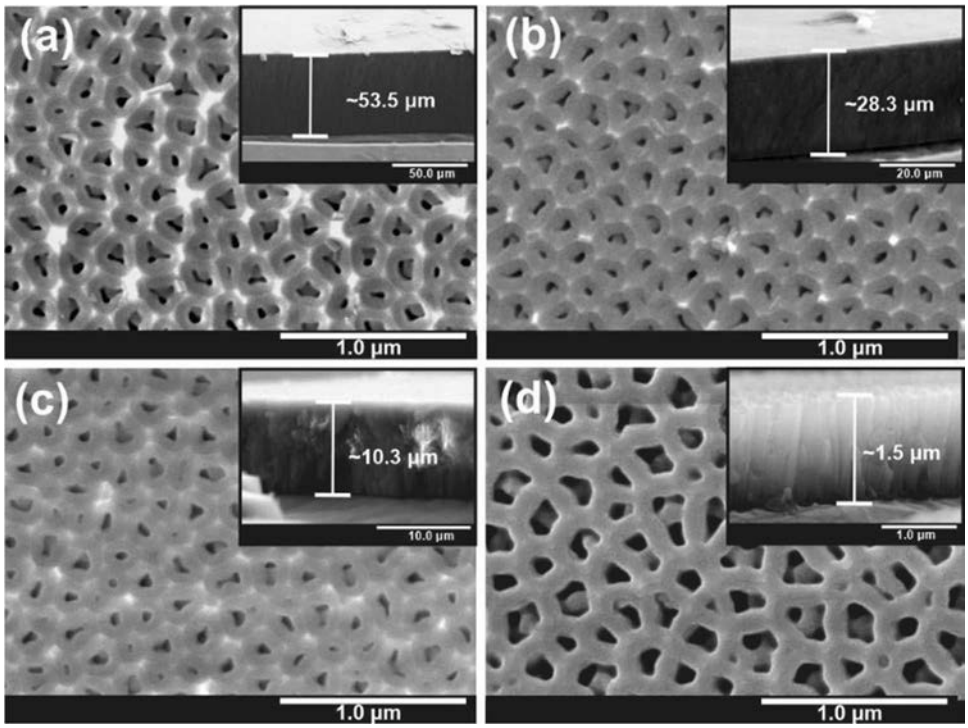

Fig. 4 FE-SEM images of AAO layers grown by two-step anodization in the electrolyte containing 0.3 M $H_2C_2O_4$ (**a**), 0.25 M $H_2C_2O_4$ and 0.05 M H_3PO_4 (**b**), 0.2 M $H_2C_2O_4$ and 0.1 M H_3PO_4 (**c**), and 0.3 M H_3PO_4 (**d**) at the potential of 80 V (cross-sectional views shown as insets)

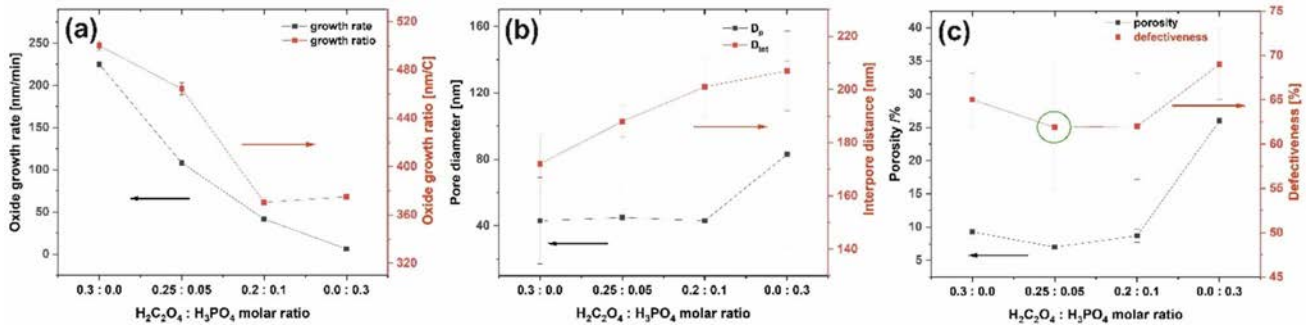

Fig. 5 The values of oxide growth rate and oxide growth ratio (**a**), average pore diameter and interpore distance (**b**), average porosity and percentage of defective pores (**c**) calculated for porous AAO layers grown in electrolytes of different content of $H_2C_2O_4$ and H_3PO_4 at 80 V

(Fig. 5c). Similarly, such an addition of phosphoric acid did not affect the values of channel diameters and porosity.

The morphology of the bottom sides of the AAO layers grown at selected conditions was also evaluated (see Fig. S2 in the Supplementary Information). As can be seen, a noticeable higher degree of pore order (lower defectiveness) is observed at the bottom side of the anodic film (Fig. S2e) independently of the conditions applied. This is in line with expectations, since the outer oxide film, grown at the beginning of the process is susceptible to mechanical deformation and mostly, field-assisted etching by the electrolyte over a longer time. Moreover, similar values of D_{int} were observed on the top and the bottom side of the AAO layers grown at the potential of 40 V in pure $H_2C_2O_4$ (Fig. S2f) since hexagonally ordered and vertically aligned channels are obtained at these conditions. On the contrary, larger cell sizes are observed from the bottom side of the anodic films obtained at 80 V which can be explained by the lower regularity of the outer layer and, sometimes, the formation of smaller subpores [47], as can be seen in Fig. 4.

Anodization of Al in H_2SO_4 – H_3PO_4 mixtures

The second mixture tested was a mixture of sulfuric and oxalic acids. As already mentioned, to the best of our knowledge, the use of this kind of electrolyte for Al anodizing has not been reported so far. First, 25 V was selected as the anodizing voltage, since it is well-known to be the self-ordering regime for pure H_2SO_4. Figure S3a (see Supplementary Information) shows the current curves recorded in electrolyte solutions of different compositions based on these acids. The observed trends are similar to those in the case of anodization in solutions based on oxalic acid. The presence of phosphoric acid significantly reduces the current density and causes the local minimum and maximum indicating the moment of the beginning of pore formation and their reorganization, respectively to appear later. Moreover, in the case of pure phosphoric acid and solutions with the lowest tested sulfuric acid content, the current curves do not exhibit any local extremes.

SEM images of AAO layers obtained in different electrolytes containing H_2SO_4 and/or H_3PO_4 at 25 V are collected in Fig. 6. The consequences of lower current density values observed when using electrolytes with a higher phosphoric acid content (Fig. S3a) are lower rates of oxide layer growth (Fig. 7a). Similarly, for higher phosphoric acid concentrations, a gradual increase in pore diameters, inter-pore distances and porosity is observed (Fig. 7b and c). Considering that the growth efficiency decreases with increasing H_3PO_4 concentration (Fig. 7a) with a simultaneous increase in porosity (decrease in oxide layer density) (Fig. 7c), it may suggest more effective oxide etching by electrolytes containing phosphoric acid, as well as the possibility of competitive processes occurring at the same potential, such as oxygen co-evolution, as already suggested by some previous works [42, 43].

Similarly to the previous mixture, also in this case a clear deterioration of the degree of pore order was observed

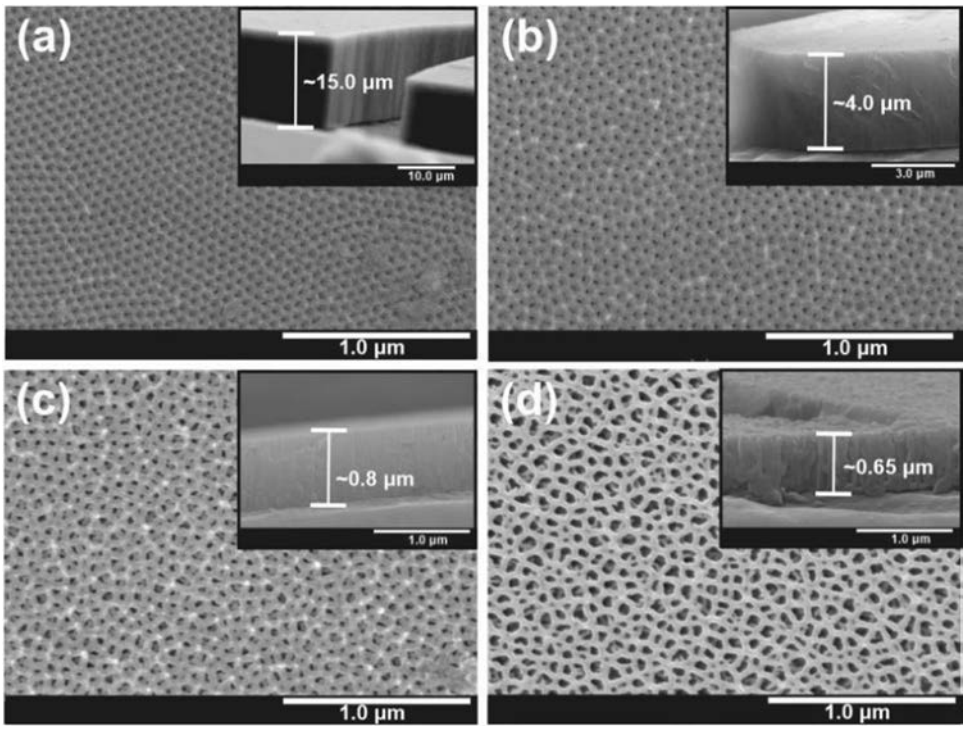

Fig. 6 FE-SEM images of AAO layers grown by two-step anodization in the electrolyte containing 0.3 M H_2SO_4 (**a**), 0.2 M H_2SO_4 and 0.1 M H_3PO_4 (**b**), 0.1 M H_2SO_4 and 0.2 M H_3PO_4 (**c**), and 0.3 M H_3PO_4 (**d**) at the potential of 25 V (cross-sectional views shown as insets)

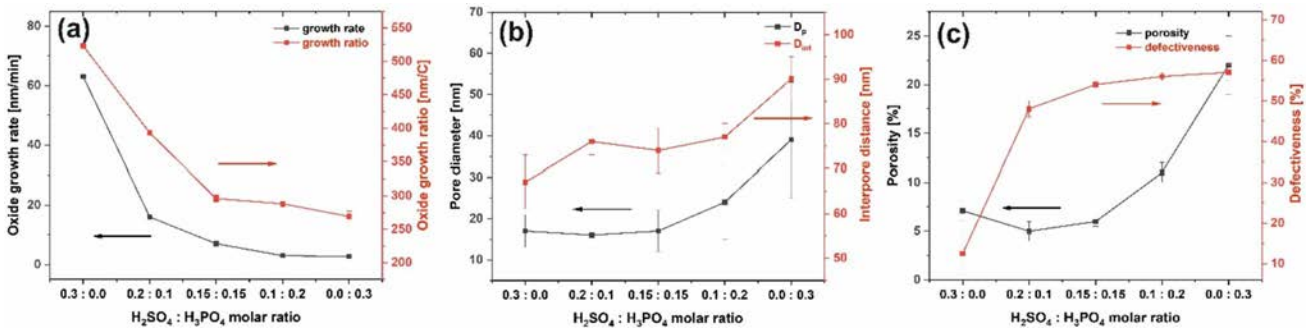

Fig. 7 The values of oxide growth rate and oxide growth ratio (**a**), average pore diameter and interpore distance (**b**), average porosity and percentage of defective pores (**c**) calculated for porous AAO layers grown in electrolytes of different content of H_2SO_4 and H_3PO_4 at 25 V

(higher percentage of defective pores, greater inhomogeneities of diameters and distances between pores) after the addition of phosphoric acid, which is of course in line with expectations. When pure H_2SO_4 was applied as an electrolyte, ordered hexagonal domains with clear boundaries between them were clearly visible (Fig. 6a), similar to those observed in previous works [46, 48]. The same trends were observed comparing the morphologies of the bottom sides of the AAO layers (Fig. S4 in the Supplementary Information).

Anodization was also carried out at 30 V, i.e. at a voltage that is hard to apply for pure H_2SO_4 in most cases due to uncontrolled dissolution of the metal. SEM images of layers obtained in electrolytes with different phosphoric acid contents are shown in Fig. 8. It is clearly visible that slightly thicker layers were obtained than for a potential of 25 V for the same electrolytes, which is in line with expectations (Fig. S5 in the Supplementary Information). Also in this case, the more phosphoric acid in the electrolyte, the lower the oxide growth rates, but the growth efficiency is higher (Fig. 9a), which may suggest that going beyond the self-ordering regime to higher voltages for higher sulfuric acid contents may result in more effective dissolution of the oxide layer. Similarly, the distance between channels decreases with the addition of phosphoric acid, but the channel diameter and porosity increase (Fig. 9b and c). Also for a voltage of 30 V, the highest degree of pore ordering was observed when using an electrolyte with the highest sulfuric acid content (Fig. 9c).

Finally, the exact reasons behind the trends observed in both $H_2C_2O_4$ and H_2SO_4-based electrolytes after introducing H_3PO_4 are not fully clear, and several aspects should be considered to explain the observed phenomena. Firstly, the barrier layer thickness formed at the pore bottoms is thinner when anodization is carried out in phosphoric acid compared to the oxalic and sulfuric acid electrolytes [11]. Secondly, the presence of phosphate ions in the electrolyte results in different efficiencies of the incorporation of anionic species to alumina structure leading to the formation of duplex or even triplex structure of cell wall within the anodic layer [49]. In consequence, the field-assisted dissolution of the oxide film is enhanced in the electrolyte containing phosphoric acid [35]. However, it should be also remembered that all geometrical features of anodic layers (including barrier layer thickness), the amount of anionic species incorporated, and properties of the AAO layers also strongly depend on other anodizing conditions such as applied voltage, temperature, and electrolyte concentration to mention only the most important ones [11]. Moreover, it was also postulated that the formation of characteristic serrated nanopores during Al anodization in H_3PO_4 electrolytes

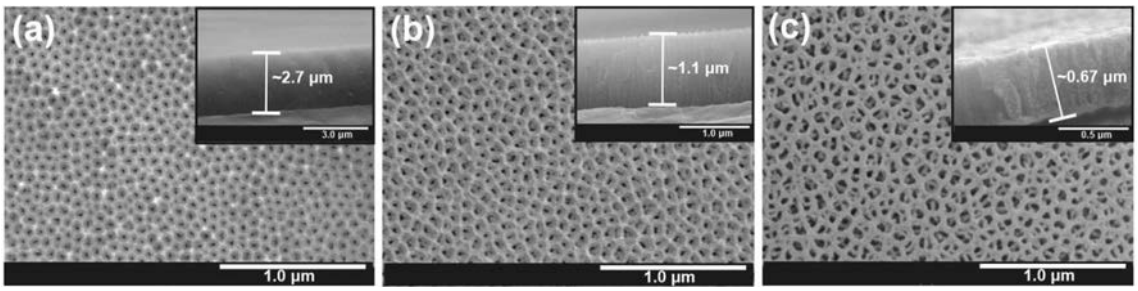

Fig. 8 FE-SEM images of AAO layers grown by two-step anodization in the electrolyte containing 0.15 M H_2SO_4 and 0.15 M H_3PO_4 (**a**), 0.1 M H_2SO_4 and 0.2 M H_3PO_4 (b) and 0.3 M H_3PO_4 at the potential of 30 V (cross-sectional views shown as insets)

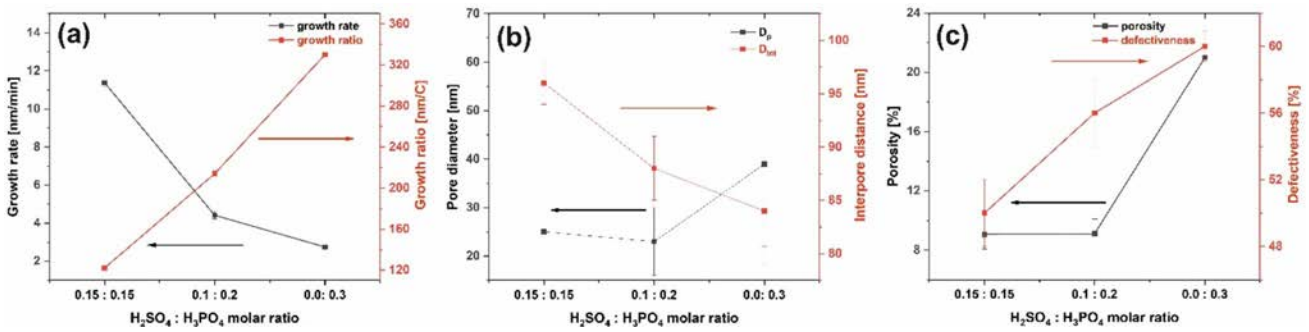

Fig. 9 The values of oxide growth rate and oxide growth ratio (**a**), average pore diameter and interpore distance (**b**), average porosity and percentage of defective pores (**c**) calculated for porous AAO layers grown in electrolytes of different content of H_2SO_4 and H_3PO_4 at 30 V

is a result of O_2 bubble evolution and plastic deformation of the anodic film [43]. Nevertheless, some further studies are still mandatory to unravel the influence of various factors and fully understand the mechanisms behind the effect of phosphoric acid content on the growth and morphology of porous AAO layers.

Conclusions

In summary, it can be stated that the use of a mixture of different acids instead of a solution of single acid as an electrolyte for Al anodization provides another degree of freedom to control both the kinetics of oxide layer growth as well as the geometrical features of the resulting AAO films. In particular, when the anodization is carried out in oxalic acid-based electrolytes at voltages close to the self-ordering regime (relatively close to 40 V), the addition of H_3PO_4 results in a significant decrease in oxide growth rate, while the values of pore diameter and interpore distance are not as much affected if only the $H_2C_2O_4$ is present in the electrolyte. Nevertheless, the degree of pore order and uniformity of the pore distribution and size increase significantly with increasing H_3PO_4 content in the electrolyte. On the contrary, when a higher voltage is applied (far from the self-ordering regime) a noticeable increase in pore ordering can be achieved by the addition of a small amount of H_3PO_4 to $H_2C_2O_4$. Finally, as was proved, an addition of H_3PO_4 to H_2SO_4 makes it possible to successfully perform anodization of Al even at 30 V without burning phenomena, and the morphology of AAO film is also strongly dependent on the composition of H_3PO_4–H_2SO_4 electrolyte. It is strongly believed that careful adjustment of the composition of acid mixtures can be another valuable tool for fine-tuning the geometry of porous alumina layers.

Supplementary Information The online version contains supplementary material available at https://doi.org/10.1007/s10008-024-06114-y.

Acknowledgements The research was supported by the National Science Centre Poland (Contract No. UMO-2018/30/E/ST5/00531). The SEM imaging was performed in the Laboratory of Field Emission Scanning Electron Microscopy and Microanalysis at the Institute of Geological Sciences, Jagiellonian University, Poland.

Authors' contribution Conceptualization: [AŚ, LZ]; Methodology: [AŚ, LZ]; Formal analysis and investigation: [AŚ]; Writing - original draft preparation: [AŚ]; Writing - review and editing: [LZ]; Funding acquisition: [LZ]; Resources: [AŚ, LZ]; Supervision: [LZ].

References

1. Sulka GD, Zaraska L, Stępniowski WJ (2011) In: Nalwa HS (ed) Encyclopedia of nanoscience and nanotechnology, 2nd edn. American Scientific
2. Ruiz-Clavijo A, Caballero-Calero O, Martín-González M (2021) Revisiting anodic alumina templates: from fabrication to applications. Nanoscale 13:2227–2265. https://doi.org/10.1039/D0NR07582E
3. De Graeve I, Laha P, Goossens V, Furneaux R, Verwimp D, Stijns E, Terryn H (2011) Colour simulation and prediction of complex nano-structured metal oxide films: test case: analysis and modeling of electro-coloured anodized aluminium. Surf Coat Technol 205:4349–4354. https://doi.org/10.1016/j.surfcoat.2011.03.018
4. Itoh H, Yanagishita T (2024) Anodic porous alumina membranes with chemical stability improved by atomic layer deposition coating of TiO2. ECS J Solid State Sci Technol 13:023002. https://doi.org/10.1149/2162-8777/ad2197

5. Santos A, Kumeria T, Losic D (2013) Nanoporous anodic aluminum oxide for chemical sensing and biosensors. TRAC Trends Anal Chem 44:25–38. https://doi.org/10.1016/j.trac.2012.11.007
6. Yamashita T, Kodama S, Ohto M, Nakayama E, Takayanagi N, Kemmei T, Yamaguchi A, Teramae N, Saito Y (2007) Use of porous anodic alumina membranes as a nanometre-diameter column for high performance liquid chromatography. Chem Commun 1160–1162. https://doi.org/10.1039/B615369K
7. Aw MS, Bariana M, Losic D (2015). In: Losic D, Santos A (eds) Nanoporous alumina fabrication, structure, properties and applications, 1st edn. Springer Cham. https://doi.org/10.1007/978-3-319-20334-8_11
8. Losic D, Santos A (eds) (2015) Nanoporous alumina. fabrication, structure, properties and applications, 1st edn. Springer Cham. https://doi.org/10.1007/978-3-319-20334-8
9. Lee W, Park SJ (2014) Porous anodic aluminum oxide: anodization and templated synthesis of functional nanostructures. Chem Rev 114:7487–7556. https://doi.org/10.1021/cr500002z
10. Sulka GD (ed) (2020) Nanostructured anodic metal oxides, synthesis and applications, 1st edn. Elsevier, Amsterdam
11. Sulka GD (2008). In: Eftekhari A (ed) Nanostructured materials in electrochemistry, 1st edn. Wiley-VCH. https://doi.org/10.1002/9783527621507
12. Zaraska L, Stępniowski WJ, Jaskuła M, Sulka GD (2014) Analysis of nanopore arrangement of porous alumina layers formed by anodizing in oxalic acid at relatively high temperatures. Appl Surf Sci 305:650–657. https://doi.org/10.1016/j.apsusc.2014.03.154
13. Asoh H, Matsumoto M, Hashimoto H (2019) Effects of ethanol on the efficiency of the formation of anodic alumina in sulfuric acid. Surf Coat Technol 378:124947. https://doi.org/10.1016/j.surfcoat.2019.124947
14. Li SY, Wang J, Li Y, Zhang X, Wang G, Wang C (2014) Photoluminescent properties of anodic aluminum oxide films formed in mixture of malonic and sulfuric acid. Superlattice Microstruct 75:294–302. https://doi.org/10.1016/j.spmi.2014.07.018
15. Lu J, Wei G, Yu Y, Guo C, Jiang L (2018) Aluminum alloy AA2024 anodized from the mixed acid system with enhanced mechanical properties. Surf Interfaces 13:46–50. https://doi.org/10.1016/j.surfin.2018.08.003
16. Mohammadniaei M, Maleki K, Kashi MA, Ramezani A, Mayamei Y (2016) Self ordered nanopore arrays through hard anodization assisted by anode temperature ramp. Appl Phys A 122:195. https://doi.org/10.1007/s00339-016-0446-4
17. Barzegar S, Absalan G, Moradi M, Behaein S (2020) Constructing geometrically-ordered alumina nanoporous filters and alumina nanowire arrays by using ultrahigh voltage two step anodization. Phys E Low Dimens Syst Nanostruct 117:113789. https://doi.org/10.1016/j.physe.2019.113789
18. Rayat Azimi AH, Zarei M, Rafati A, Noormohammadi M Fabrication of self-ordered nanoporous alumina with 500–750 nm interpore distances using hard anodization in phosphoric/oxalic acid mixtures. J Porous Mater 23:357–363 https://doi.org/10.1007/s10934-015-0088-5
19. Xu Y, Liu H, Li X, Kang W, Cheng B, Li X (2015) A novel method for fabricating self-ordered porous anodic alumina with wide interpore distance using phosphoric/oxalic acid mixed electrolyte. Mater Lett 151:79–81. https://doi.org/10.1016/j.matlet.2015.03.049
20. Yanagishita T, Koga A, Masuda H (2023) Continuous spinning of polymer nanofibers with uniform diameters using an anodic porous alumina spinneret with holes of different diameters. Mater Adv 4:890–900. https://doi.org/10.1039/D2MA01017H
21. Kashi MA, Ramazani A (2010) Ordered nanoporous alumina membranes formed in oxalic/phosphoric acid using hard anodization. Int J Nanosci Nanotechnol 6:78–87
22. Voon CH, Lim BY, Foo KL, Hashim U, Ting SS, Arshad MK, Md, Mustafa NAI (2016) Synthesis of porous anodic alumina (PAA) on aluminum alloy AA6061 in mixture of phosphoric acid and oxalic acid. Mater Sci Forum 857:237–241. https://doi.org/10.4028/www.scientific.net/MSF.857.237
23. Kao TT, Chang YC (2014) Influence of anodization parameters on the volume expansion of anodic aluminum oxide formed in mixed solution of phosphoric and oxalic acids. Appl Surf Sci 288:654–659. https://doi.org/10.1016/j.apsusc.2013.10.091
24. Yanagishita T, Moriyasu R, Ishii T, Masuka H (2021) Self-ordered anodic porous alumina with inter-hole spacing over 1,5 μm. RCS Adv 11:3777. https://doi.org/10.1039/D0RA10269E
25. Chen X, Yu D, Cao L, Zhu X, Song Y, Huang H (2014) Fabrication of ordered porous anodic alumina with ultra-large interpore distances using ultrahigh voltages. Mater Res Bull 57:116–120. https://doi.org/10.1016/j.materresbull.2014.05.037
26. Wang J, Jiang L, Peng N, Tan Q, Liang L (2021) Effect of hydration on porous anodic alumina with large interpore distances during anodization with ultrahigh voltage. Int J Electrochem Sci 16:1–8. https://doi.org/10.20964/2021.03.04
27. Kashi MA, Ramazani A, Rahmandoust M, Noormohammadi M (2007) The effect of pH and composition of sulfuric-oxalic acid mixture on the self-ordering configuration of high porosity alumina nanohole arrays. J Phys D Appl Phys 40:4625–4630. https://doi.org/10.1088/0022-3727/40/15/040
28. Kashi MA, Ramazani A, Mayamai Y, Noormohammadi M (2010) Fabrication of self-ordered nanoporous alumina with 69–115 nm interpore distances in sulfuric/oxalic acid mixtures by hard anodization. Jpn J Appl Phys 49:015202. https://doi.org/10.1143/JJAP.49.015202
29. Shingubara S, Morimoto K, Sakaue H, Takahagi T (2004) Self-organization of a porous alumina nanohole array using a sulfuric/oxalic acid mixture as electrolyte. Electrochem Solid-State Lett 7:E15–E17. https://doi.org/10.1149/1.1644353
30. Roslyakov IV, Kolesnik IV, Belokozenko MA, Yapryntsev AD, Napolskii KS (2023) Thermal transformations of porous anodic aluminum oxide formed in Sulfuric Acid/Oxalic acid mixed Electrolytes. Russ J Inorg Chem 68:923–930. https://doi.org/10.1134/S003602362360079X
31. Choudhari KS, Kulkarni SD, Santhosh C, George SD (2018) Influence of electrolyte composition on the photoluminescence and pore arrangement of nanoporous anodic alumina. ECS J Solid State Sci Technol 7:R175–R182. https://doi.org/10.1149/2.0081811jss
32. Zhao L, Wang J, Li Y, Wang C, Zhou F, Liu W (2010) Anodic aluminum oxide films formed in mixed electrolytes of oxalic and sulfuric acid and their optical constants. Phys B Condens Matter 405:456–460. https://doi.org/10.1016/j.physb.2009.08.306
33. Kashi MA, Ramazani A, Noormohammadi M, Zarei M, Marashi P (2007) Optimum self-ordered nanopore arrays with 130–270 nm interpore distances formed by hard anodization in sulfuric/oxalic acid mixtures. J Phys D Appl Phys 40:7032–7040. https://doi.org/10.1088/0022-3727/40/22/025
34. Li J, Li C, Chen C, Hao Q, Wang Z, Zhu J, Gao X (2012) Facile method for modulating the profiles and periods of self-ordered three-dimensional alumina taper-nanopores. ACS Appl Mater Interfaces 4:5678–5683. https://doi.org/10.1021/am301603e
35. Yanagishita T, Kawato R, Masuda H (2022) Highly ordered anodic porous alumina prepared by anodization of Al in extremely dilute H_2SO_4. J Electrochem Soc 169:073504. https://doi.org/10.1149/1945-7111/ac7dc9
36. Rasband IWS (1997–2014) ImageJ, US National Institutes of Health, Bethesda, Maryland, USA. http://imagej.nih.gov/ij/. Accessed 25 Jul 2024

37. Horcas I, Fernández R, Gómez-Rodríguez JM, Colchero J, Gómez-Herrero J, Baro AM (2007) WSXM: a software for scanning probe microscopy and a tool for nanotechnology. Rev Sci Instrum 78:013705. https://doi.org/10.1063/1.2432410
38. Ciepiela E, Zaraska L, Sulka GD (2012). In: Bubak M, Szepieniec T, Wiatr K (eds) Building a national distributed e-Infrastructure–PL-Grid. Lecture notes in computer science, 1st edn. Springer, Berlin, Heidelberg. https://doi.org/10.1007/978-3-642-28267-6_19
39. Zaraska L, Stępniowski WJ, Ciepiela E, Sulka GD (2013) The effect of anodizing temperature on structural features and hexagonal arrangement of nanopores in alumina synthesized by two-step anodizing in oxalic acid. Thin Solid Films 534:155–161. https://doi.org/10.1016/j.tsf.2013.02.056
40. Li F, Zhang L, Metzger RM (1998) On the growth of highly ordered pores in anodized aluminum oxide. Chem Mater 10:2470–2480. https://doi.org/10.1021/cm980163a
41. Zaraska L, Brudzisz A, Wierzbicka E, Sulka GD (2016) The effect of electrolyte change on the morphology and degree of nanopore order of porous alumina formed by two-step anodization. Electrochim Acta 198:259–267. https://doi.org/10.1016/j.electacta.2016.03.050
42. Li D, Jiang C, Jiang J, Lu JG (2009) Self-assembly of periodic serrated nanostructures. Chem Mater 21:253–258. https://doi.org/10.1021/cm8022242
43. Li D, Zhao L, Jiang C, Lu JG (2010) Formation of anodic aluminum oxide with serrated nanochannels. Nano Lett 10:2766–2771. https://doi.org/10.1021/nl1004493
44. Zaraska L, Stępniowski WJ, Sulka GD, Ciepiela E, Jaskuła M (2014) Analysis of nanopore arrangement and structural features of anodic alumina layers formed by two-step anodizing in oxalic acid using the dedicated executable software. Appl Phys A 114:571–577. https://doi.org/10.1007/s00339-013-7618-2
45. Zaraska L, Sulka GD, Szeremeta J, Jaskuła M (2010) Porous anodic alumina formed by anodization of aluminum alloy (AA1050) and high purity aluminum. Electrochim Acta 55:4377–4386. https://doi.org/10.1016/j.electacta.2009.12.054
46. Sulka GD, Parkoła KG (2006) Anodizing potential influence on well-ordered nanostructures formed by anodization of aluminium in sulphuric acid. Thin Solid Films 515:338–345. https://doi.org/10.1016/j.tsf.2005.12.094
47. Zaraska L, Sulka GD, Jaskuła M (2010) The effect of n-alcohols on porous anodic alumina formed by self-organized two-step anodizing of aluminum in phosphoric acid. Surf Coat Technol 204:1729–1737. https://doi.org/10.1016/j.surfcoat.2009.10.051
48. Sulka GD, Jaskuła M (2006) Defect analysis in self-organized nanopore arrays formed by anodization of aluminium at various temperatures. J Nanosci Nanotechnol 6:3803–3811. https://doi.org/10.1166/jnn.2006.617
49. Ono S, Ichinose H, Masuko N (1992) The high resolution observation of porous anodic films formed on aluminum in phosphoric acid solution. Corr Sci 33:841–850